# Estimating the vertical electron density profile from an ionogram: On the passage from true to virtual heights via the target function method

C. Scotto,[1,2] M. Pezzopane,[1] and B. Zolesi[1]

Received 20 July 2011; revised 24 November 2011; accepted 30 November 2011; published 28 January 2012.

[1] The paper describes a new simple method of calculation by which an artificial ionogram trace is obtained from a given vertical electron density profile. The method is discussed in terms of the target function method used by Autoscala to output a reliable estimation of the real vertical electron density profile associated to the recorded ionogram. This new approach solves the issue of the pole in the calculation of virtual height, and consequently eliminates all the divergence phenomena that sometimes characterized the artificial ionogram traces computed by Autoscala. In contrast to the POLAN procedure, the technique introduced in this paper to pass from true to virtual heights is not based on any arithmetical operation related to changes of integration variables. Since the target function method on which Autoscala is based requires that the passage from a vertical electron density profile to an artificial ionogram be repeated a very large number of times, this new calculation procedure is advantageous in terms of speeding up the associated processing time.

**Citation:** Scotto, C., M. Pezzopane, and B. Zolesi (2012), Estimating the vertical electron density profile from an ionogram: On the passage from true to virtual heights via the target function method, *Radio Sci.*, *47*, RS1007, doi:10.1029/2011RS004833.

## 1. Introduction

[2] Ionospheric observations are performed using a high-frequency radar known as an ionosonde. The ionosonde sends short pulses of radio energy vertically into the ionosphere. These pulses are reflected back toward the ground and the ionosonde records the time delay between transmission and reception of pulses. By varying the carrier frequency of pulses, typically from 1 to 20 MHz, the time delay at different frequencies is recorded. This record is referred to as an ionogram and is usually presented in the form of a graph, where normally in place of time delay the virtual (or apparent) height is plotted according to the following equation

$$T = \frac{2}{c} h', \tag{1}$$

where $T$ is the time delay, $h'$ is the virtual height and $c$ is the free-space speed of the electromagnetic wave.

[3] The virtual height $h'$, at a specified frequency of the pulses, is then the distance that a radio wave would have traveled at that frequency in half the elapsed time, $T/2$, at the free-space speed $c$.

[4] Radio pulses travel more slowly within the ionosphere than in free space, with the group velocity $v_g < c$, and so the virtual height is greater than the true height. The difference between true height and virtual height is governed by the degree of ionization that the electromagnetic wave has passed through. Recreating the true height vertical electron density profile $N(h)$ from ionogram data is an important use of ionosonde data, in a procedure known as "true height analysis."

[5] Several methods have been developed to accomplish this task [*Wright et al.*, 1972; *Reinisch and Huang*, 1983; *Titheridge*, 1985, 1988; *Zabotin et al.*, 2006]. In any case, all the methods encounter a problem involving the divergence of the group refractive index $\mu'$ near the height of reflection. As we shall see in section 2, this problem has been addressed and solved by *Titheridge* [1985], by two changes of variable.

[6] Recently, a possible alternative solution to the problem of ionogram inversion has been described in detail by *Scotto* [2009] who used a technique in which the root mean square error between the ionogram trace restored from a candidate $N(h)$, and the real recorded trace is minimized, such an approach being similar to the function approximation methods used in many branches of applied mathematics and computer science. This method shall be briefly reviewed in section 3. In that section we will see among other things, that there is a need to compute many times the simulated ionogram from a candidate $N(h)$. This article discusses such a calculation and describes how the divergence problem of $\mu'$ has been solved by a technique optimizing the height integration step. Using this technique at the same time we optimize the process improving the computation time.

## 2. The Polynomial Method

[7] POLAN (POLynomial ANalysis), is a program [*Titheridge*, 1985] to derive $N(h)$ from the recorded trace

[1]Istituto Nazionale di Geofisica e Vulcanologia, Rome, Italy.
[2]Doctoral School in Polar Sciences, University of Siena, Siena, Italy.


0048-6604/12/2011RS004833

in an ionogram. Although, originally, the actual use of the inversion was performed manually, the author was already clear that an ideal procedure should provide consistent results even without the intervention of an operator. POLAN is based on an accurate, flexible procedure with adaptable resolution and has the ability to mix physically consistent conditions with the observed data, providing a weighted least squares solution.

[8] In calculating the coefficients of this polynomial approximation the problem arises of calculating the excess time delay $\Delta$ due to the ionosphere, which effectively is

$$\Delta = \int_{h_b}^{h_r} (\mu' - 1)\mathrm{d}h, \tag{2}$$

where the integration variable is the true height $h$, with $h_r$ and $h_b$ representing respectively the true height of reflection and the height of the base of the ionosphere. By changing the integration variable first to the plasma frequency $f_p$ and then to the variable

$$x^2 = 1 - \frac{f_p^2}{f_r^2}, \tag{3}$$

where $f_r$ represents the plasma frequency of reflection (which is equal to the frequency $f$ of the ordinary mode of propagation of the electromagnetic wave), equation (2) becomes

$$\Delta = \int_1^0 (\mu' - 1)\cdot \frac{\mathrm{d}h}{\mathrm{d}f_p}\cdot\frac{\mathrm{d}f_p}{\mathrm{d}x}\mathrm{d}x. \tag{4}$$

[9] By deriving $\mathrm{d}f_p/\mathrm{d}x = -(f_r^2/f_p)x$ from (3), equation (4) then becomes

$$\Delta = -\int_1^0 (\mu' - 1)\cdot \frac{\mathrm{d}h}{\mathrm{d}f_p}\cdot\frac{f_r^2}{f_p}x\mathrm{d}x$$

$$= f_r^2 \int_0^1 (\mu' - 1)\cdot \frac{\mathrm{d}h}{\mathrm{d}f_p}\cdot\frac{1}{f_p}x\mathrm{d}x. \tag{5}$$

As a result, $\Delta$ can be calculated by numerical integration, the two changes of variable making it possible for POLAN to avoid the pole in the calculation of virtual height, while a special subroutine called GIND [*Titheridge*, 1985] provides the value of $(\mu' - 1)$ accurately.

## 3. The Target Function Method

[10] The ionogram inversion by the method of the target function is performed by calculating the trace of the ionogram, from a candidate $N(h)$, and by minimizing the root mean square error between the recorded and the restored traces [*Scotto*, 2009]. This approach is similar to the function approximation methods that are used in many branches of applied mathematics. In these methods the approximation problems are solved by selecting a particular function belonging to a class that approximates a *target function* (hence the name of the method) in a task-specific way.

[11] Therefore, in the target function method it is necessary to develop an $N(h)$ model, which is able to well describe all the different physically possible situations by varying a number of input parameters.

[12] Initially, the data necessary for running the profile model is acquired. This is: the smoothed sunspot number $R_{12}$, the geomagnetic and geographic coordinates, the critical frequency *fo*F2 of the F2 layer, the Maximum Usable Frequency on a distance of 3000 km, the information regarding the presence of F1 layer, and in the case, the associated critical frequency *fo*F1.

[13] Then, a large set of profiles of electron density is generated, for each of which an artificial associated ionogram will be computed and compared with the trace of the ionogram actually measured. Among all the generated profiles, the one associated to the ionogram having the best fit to the trace recorded by the ionosonde is selected. It is therefore understandable that the application of this method needs to repeatedly perform the numerical integration leading to the reflection virtual height calculation, which will be described in detail in the following section.

## 4. From a Vertical Electron Density Profile to the Corresponding Ionogram in Target Function Method: The Proposed Technique to Improve the Numerical Calculation

[14] The relation (1) can be written as

$$h' = \int_0^T \frac{c}{2}\mathrm{d}t, \tag{6}$$

where the integration variable is the time $t$; since the group velocity $v_g$ at which the energy of the signal travels is related to the velocity of light $c$ as

$$v_g = \frac{c}{\mu'}, \tag{7}$$

by deriving $c$ from (7) and substituting it in (6) we get

$$h' = \int_0^T \frac{\mu' v_g}{2}\mathrm{d}t. \tag{8}$$

Since $\mathrm{d}h/\mathrm{d}t = v_g$, equation (8) becomes

$$h' = \int_0^{h_r} \mu'\mathrm{d}h. \tag{9}$$

Since below the base of the ionosphere $\mu' = 1$, equation (9) can be finally written as

$$h' = h_b + \int_{h_b}^{h_r} \mu'\mathrm{d}h. \tag{10}$$

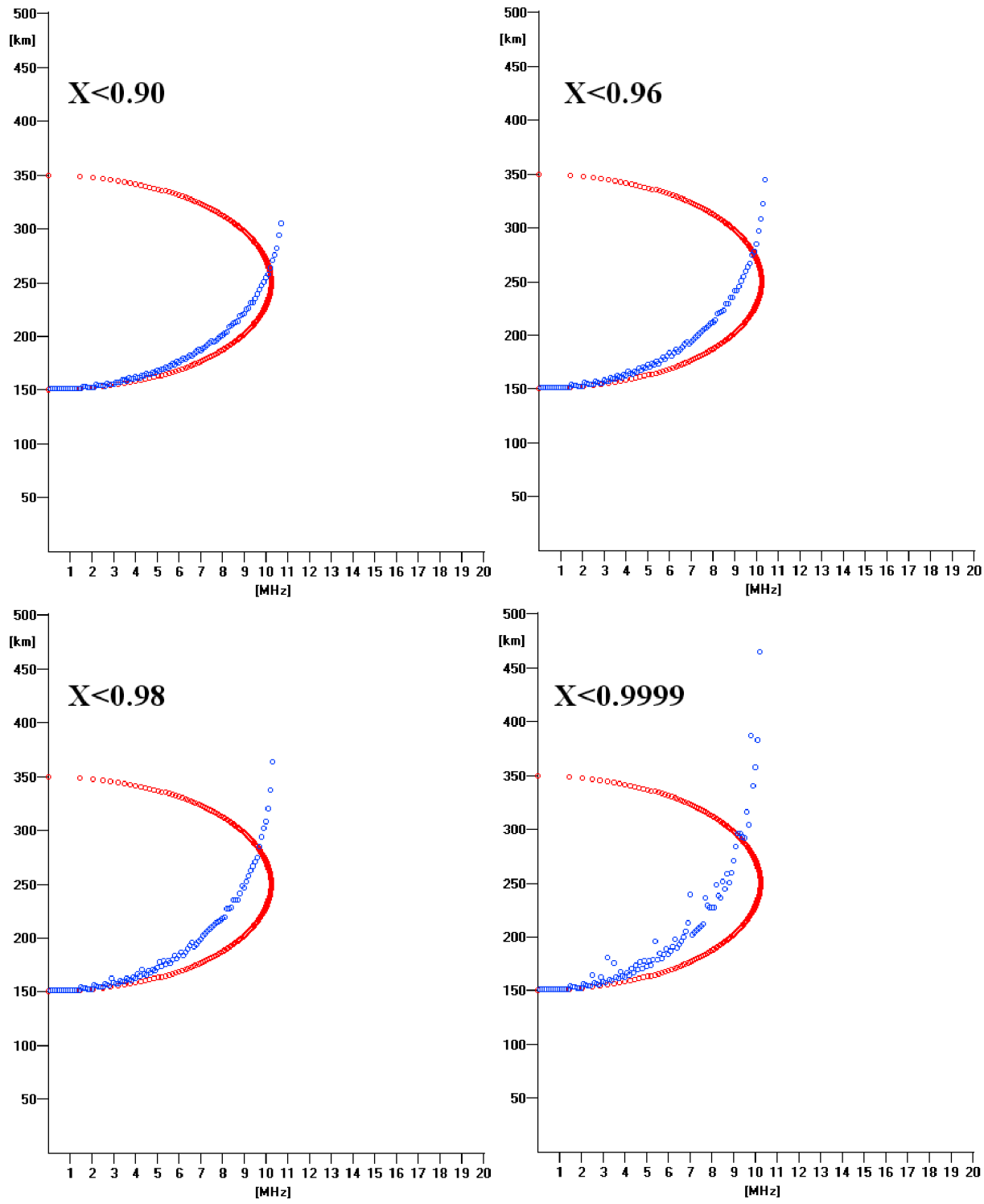


**Figure 1.** Computed ionogram (in blue) obtained by numerically computing equation (13) with $h_b = 150$ km and $\delta h = 1$ km, by considering the parabolic layer (14) (in red) with $N_0 = 1.3 \cdot 10^{12}$ electrons/m$^3$, $h_0 = 250$ km, and $D = 100$ km, and by performing the calculation for $X < \tau$ with $\tau = 0.90$, 0.96, 0.98, and 0.9999 respectively.

[15] In general, $\mu'$ depends on the frequency of the radio wave, on the direction $\theta$ of propagation with respect to the geomagnetic field and on some properties of the ionospheric medium, like electron density and magnetic field strength, expressed through the plasma frequency and the electron gyrofrequency. However, if

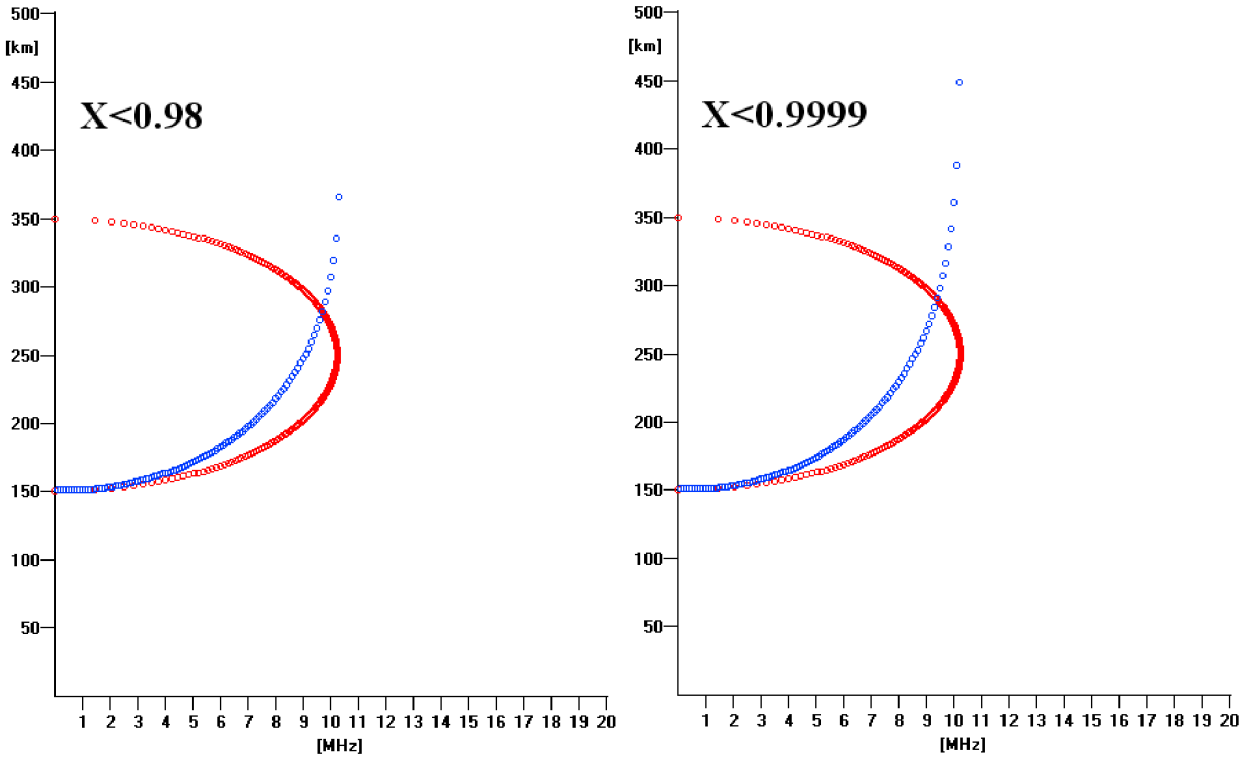


**Figure 2.** Computed ionogram (in blue) obtained by numerically computing equation (15) with $h_b$ = 150 km and $s$ = 1 km, by considering the parabolic layer (14) (in red) with $N_0 = 1.3 \cdot 10^{12}$ electrons/m$^3$, $h_0$ = 250 km, and $D$ = 100 km, and by performing the calculation fixing $\tau$ = 0.98 and 0.9999 respectively.

both the effect of the magnetic field of the Earth and the collisions of electrons with neutral particles and ions are neglected, the following relation holds for the group refractive index:

$$\mu' = \frac{1}{\mu} = \frac{1}{\sqrt{1-X}} = \frac{1}{\sqrt{1-\frac{\omega_p^2}{\omega^2}}} = \frac{1}{\sqrt{1-\frac{N(h)e^2}{4\pi^2\varepsilon_0 m f^2}}}, \qquad (11)$$

where $\mu$ is the phase refractive index, $\omega_p$ is the angular plasma frequency, $\omega$ and $f$ are respectively the angular frequency and the frequency of the electromagnetic wave, $N(h)$ is the electron density function of the true height, $e$ and $m$ are respectively the charge and the mass of the electron, and $\varepsilon_0$ is the permittivity of free space.

[16] By substituting (11) in (10) we finally obtain

$$h' - h_b = \int_{h_b}^{h_r} \mu'(h)\mathrm{d}h = \int_{h_b}^{h_r} \frac{1}{\sqrt{1-\frac{N(h)e^2}{4\pi^2\varepsilon_0 m f^2}}}\mathrm{d}h. \qquad (12)$$

(12) represents the integral by which, given a definite $N(h)$, the corresponding simulated ionogram trace $h'(f)$ can be calculated. In fact, assuming that $\mu'$ is constant over short intervals of $h$, the integral in (12) can be replaced by the following summation over $i$

$$h' = h_b + \sum_{i=1}^{p} \mu'(h_i)\delta h, \qquad (13)$$

and the summation (13) can now be numerically computed by considering definite true height intervals.

[17] From the expression (11) it is clear that, given a radio wave of frequency $f$, approaching the height of reflection with increasing the value of $N$, $X = \omega_p^2/\omega^2$ tends to 1 and consequently the quantity $\mu'$ tends to infinity; hence, in order to avoid divergences in the calculation, we have to set for $X$ a threshold $\tau$ lower than 1 above which the calculation stops. In other words, $p$ appearing in (13) is numerically defined through the relations $X(h_p) < \tau$ and $X(h_{p+1}) \geq \tau$. Of course, in order to have a realistic virtual height of reflection, this threshold has to be as close as possible to 1.

[18] Consider for example the following simple parabolic ionospheric layer:

$$\begin{cases} N(h) = N_0\left[1 - \left(\frac{h-h_0}{D}\right)^2\right] & \text{if} \quad |h-h_0| < D \\ N(h) = 0 \quad \text{if} \quad |h-h_0| \geq D \end{cases}, \qquad (14)$$

where $N_0$ is the peak electron density at a height $h_0$, and $D$ is the half-thickness of the parabola. We use a parabolic layer only to show the issue in the simplest possible way. Indeed, the virtual height of reflection for an electron density profile with parabolic shape admits an exact solution, for which the integral (12) could be calculated without resorting to the numerical computation of the summation (13). However, in this context, it is advisable to still refer to this summation (13) for the fact that Autoscala [*Pezzopane and Scotto*, 2005, 2007; *Scotto and Pezzopane*, 2012] works with more complicated shapes of $N(h)$ [*Scotto*, 2009] and then needs to solve the integral (12) according to (13). Figure 1 shows

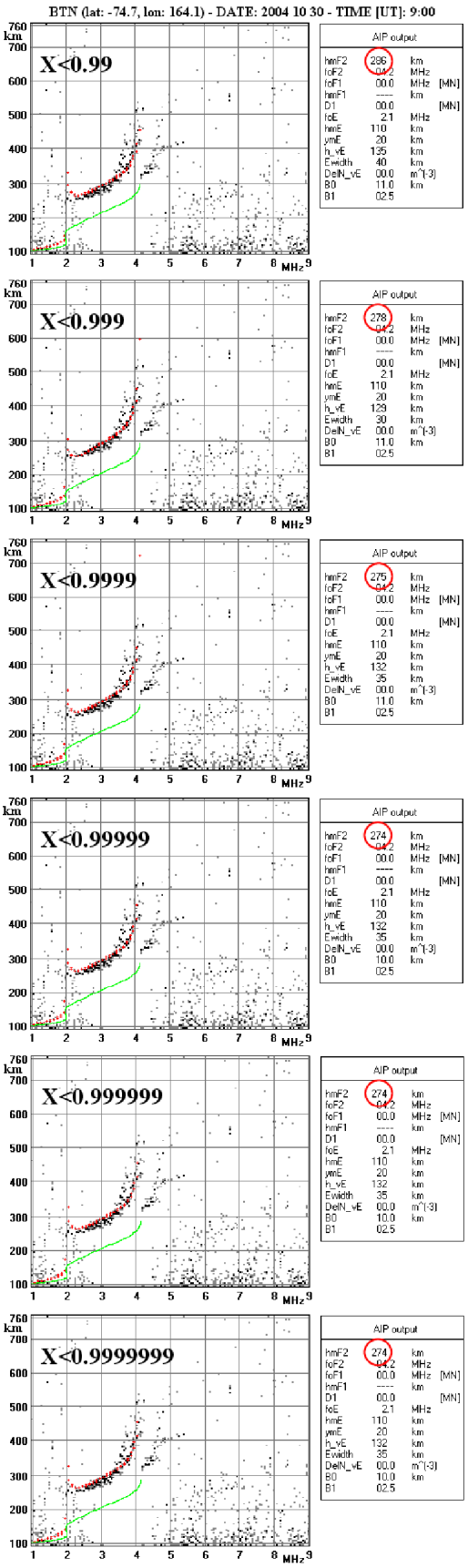


the computed ionogram obtained by numerically solving equation (13) with $h_b = 150$ km and $\delta h = 1$ km, by considering the parabolic layer (14) with $N_0 = 1.3 \cdot 10^{12}$ electrons/m$^3$, $h_0 = 250$ km, and $D = 100$ km, and by performing the calculation till $X < 0.90$, $X < 0.96$, $X < 0.98$, and $X < 0.9999$ respectively. $\tau$ is then routinely shifted closer and closer to 1 until a value for which the computed ionogram can be considered the actual $h'(f)$ trace associated to $N(h)$. It is clear from Figure 1 that by increasing $\tau$ the cusp of the computed ionogram, corresponding to the electron density peak of the layer, becomes more and more pronounced and actual. However, Figure 1 illustrates also how above a certain value the increase of $\tau$ causes significant instability in the calculation, due to divergence of $\mu'$ close to the height of reflection.

[19] This kind of unstable behavior characterizing the computed ionogram for large values of $\tau$ undoubtedly represents a significant limitation, because an obligation to maintain the value of $X$ below a definite $\tau$ could lead to an underestimation of the virtual reflection height $h'$.

[20] In order to solve this problem, we propose to compute the integral (12) as

$$h' = h_b + \sum_{i=1}^{p} \mu'(h_i)\delta h_i, \tag{15}$$

in which

$$\delta h_i = \frac{s}{\mu'(h_i)}. \tag{16}$$

[21] In practice, (15), and hence (16), mean that now the true height step $\delta h_i$ is no longer fixed but decreases as the group refractive index $\mu'$ increases, while the virtual height increments are constant and set equal to $s$. This value should be set consistently with the virtual height resolution of the ionogram. For example $s = 1$ km is an appropriate choice.

[22] Figure 2 shows the same as Figure 1 for $\tau = 0.98$ and $\tau = 0.9999$ but this time in order to compute the $h'(f)$ trace from the parabolic layer (14), summation (15) was considered instead of (13). It is again clear that by increasing $\tau$, the cusp of the computed ionogram, corresponding to the electron density peak of the layer, becomes more and more pronounced and realistic, but at the same time it is possible to see that the divergence phenomena characterizing the $h'(f)$ traces of Figure 1 are no longer present. Moreover, the processing times required to compute the $h'(f)$ traces of

**Figure 3.** Ionogram recorded at the Mario Zucchelli station, Terra Nova Bay, Antarctica, on 30 October 2004 at 9:00 UT by the AIS-INGV ionosonde and scaled by Autoscala, using equation (15), for six different values of $\tau$: 0.99, 0.999, 0.9999, 0.99999, 0.999999, and 0.9999999. In the table "AIP output," where AIP stands for Adaptive Ionospheric Profiler, the parameters used by Autoscala to estimate the vertical electron density profile associated with the reconstructed ordinary trace are shown. Considering specifically the *hm*F2 value (highlighted by a red circle), this stabilizes at a $\tau$ value equal to 0.99999.

Figure 2 were shorter than those to compute the $h'(f)$ traces of Figure 1.

## 5. The $X$ Threshold $\tau$ for the New Method of Calculation

[23] Once it had been verified that the numerical calculation based on summation (15) was much more reliable than the one based on summation (13), there remained the question as to what value should be considered for $\tau$. In order to resolve this question, Autoscala was run using a data set of ionograms recorded by the AIS-INGV ionosonde [*Zuccheretti et al.*, 2003] installed at the Mario Zucchelli station (74.7°S, 164.1°E), Terra Nova Bay, for different values of $\tau$ (0.99, 0.999, 0.9999, 0.99999, 0.999999, 0.9999999) (for the $N(h)$ used by Autoscala to compute the $h'(f)$ traces, refer to *Scotto* [2009]). Then, focusing attention on the *hm*F2 (the true height of the maximum electron density, *Nm*F2, of the F region) values given as output, the $\tau$ value was detected at which the corresponding *hm*F2 was stabilized. The meaning of this being that, if higher values of $\tau$ are considered, the corresponding values of *hm*F2 do not change by an amount greater than 1 km, which matches the virtual height increment $s$ chosen to numerically perform the summation (15).

[24] In order to facilitate understanding of this concept, an example of scaling performed by Autoscala for all the aforementioned different values of $\tau$ is shown in Figure 3. Considering specifically the *hm*F2 value, it can be seen that this stabilizes at a $\tau$ value equal to 0.99999. Hence, $X \geq 0.99999$ represents the condition under which the calculation of equation (15) stops, thereby assuring a realistic representation of the $h'(f)$ trace.

## 6. Summary

[25] This work described a simple method to numerically compute the integral for the determination of an $h'(f)$ trace from a $N(h)$. It was demonstrated how this method completely eliminates all the divergence phenomena that sometimes characterize the $h'(f)$ traces computed by Autoscala, providing a much more realistic condition of integration for the parameter $X$.

[26] It was also stressed the fact that using the target function method, Autoscala repeats iteratively the calculation of the integral to obtain the simulated ionogram from a candidate $N(h)$, which is consequently time consuming. In contrast to what *Titheridge* [1985] proposed in the framework of his polynomial analysis, in order to calculate this integral the technique here described is not based on any arithmetical operation related to changes of the integration variables. It was then also verified that this computational feature considerably speeds up the processing time required by Autoscala to calculate $h'(f)$ traces from a set of candidate vertical electron density profiles.

## References

Pezzopane, M., and C. Scotto (2005), The INGV software for the automatic scaling of foF2 and MUF(3000)F2 from ionograms: A performance comparison with ARTIST 4.01 from Rome data, *J. Atmos. Sol. Terr. Phys.*, *67*(12), 1063–1073, doi:10.1016/j.jastp.2005.02.022.

Pezzopane, M., and C. Scotto (2007), The automatic scaling of critical frequency foF2 and MUF(3000)F2: A comparison between Autoscala and ARTIST 4.5 on Rome data, *Radio Sci.*, *42*, RS4003, doi:10.1029/2006RS003581.

Reinisch, B. W., and X. Huang (1983), Automatic calculation of electron density profiles from digital ionograms: 3. Processing of bottomside ionograms, *Radio Sci.*, *18*, 477–492, doi:10.1029/RS018i003p00477.

Scotto, C. (2009), Electron density profile calculation technique for Autoscala ionogram analysis, *Adv. Space Res.*, *44*(6), 756–766, doi:10.1016/j.asr.2009.04.037.

Scotto, C., and M. Pezzopane (2012), Automatic scaling of polar ionogram, *Antarct. Sci.*, doi:10.1017/S0954102011000587, in press.

Titheridge, J. E. (1985), Ionogram analysis with the generalised program Polan, *Rep. UAG-93*, World Data Cent. A for Sol.-Terr. Phys., Boulder, Colo.

Titheridge, J. E. (1988), The real height analysis of ionograms: A generalized formulation, *Radio Sci.*, *23*(5), 831–849, doi:10.1029/RS023i005p00831.

Wright, J. W., A. R. Laird, D. Obitts, E. J. Violette, and D. McKinnis (1972), Automatic $N(h,t)$ profiles of the ionosphere with a digital ionosonde, *Radio Sci.*, *7*, 1033–1042, doi:10.1029/RS007i011p01033.

Zabotin, N. A., J. W. Wright, and G. A. Zhbankov (2006), NeXtYz: Three-dimensional electron density inversion for dynasonde ionograms, *Radio Sci.*, *41*, RS6S32, doi:10.1029/2005RS003352.

Zuccheretti, E., G. Tutone, U. Sciacca, C. Bianchi, and B. J. Arokiasamy (2003), The new AIS-INGV digital ionosonde, *Ann. Geophys.*, *46*(4), 647–659.

M. Pezzopane, C. Scotto, and B. Zolesi, Istituto Nazionale di Geofisica e Vulcanologia, Via di Vigna Murata 605, I-00143 Rome, Italy. (michael.pezzopane@ingv.it; carlo.scotto@ingv.it; bruno.zolesi@ingv.it)